Carbohydrate Polymers 84 (2011) 262–267

Contents lists available at ScienceDirect

Carbohydrate Polymers

journal homepage: www.elsevier.com/locate/carbpol

Synthesis and characterization of cellulose phosphate from oil palm empty fruit bunches microcrystalline cellulose

W.D. Wanrosli*, R. Rohaizu, A. Ghazali

School of Industrial Technology, Universiti Sains Malaysia, 11800 Pulau Pinang, Malaysia

ARTICLE INFO

Article history:
Received 16 October 2010
Accepted 15 November 2010
Available online 21 November 2010

Keywords:
Oil palm empty fruit bunch
Microcrystalline cellulose
Cellulose phosphate
Phosphorylation
Biopolymers

ABSTRACT

Phosphorylated cellulose is a biopolymer with potential use in biomaterials. The typical cellulosic raw materials used in its derivation are often wood-based. Nonetheless, cellulose can also be extracted and is readily available in large quantities from non-wood alternatives. One such viable source is empty fruit bunch fiber (OPEFB), a by-product of the oil palm industry. In this work, OPEFB cellulose phosphate (OPEFB-CP) gel was successfully synthesized from OPEFB microcrystalline cellulose using the $H_3PO_4/P_2O_5/Et_3PO_4$/hexanol procedure. The characterization of the OPEFB-CP was performed using EDX analysis, FTIR and CP/MAS ^{13}C- and ^{31}P-NMR spectroscopic analyses and provided clear evidence of successful phosphorylation. Through CP/MAS ^{13}C NMR, the distribution of the phosphate moiety among the three OH groups in the glucose residues was shown to be preferably located at the C6 position, resulting in a 53% reduction in crystallinity. Thermal stability of the OPEFB-MCC decreased upon phosphorylation.

1. Introduction

Due to the unique properties of cellulose, such as its non-toxicity, swelling ability and stability under variations in temperature and pH, various new materials have been derived from this plentiful natural compound (Dumitru, 2002; Hon, 1996). There is a renewed and growing interest in cellulose derivatives due to the inexhaustibility of the raw material, which reproduces naturally and is also cultivated by humans. Among the more prominent cellulose derivatives are cellulose acetate and carboxymethyl cellulose. This renewed interest has also led to the emergence of new cellulose derivatives, such as cellulose phosphate, which have generated substantial research attention. The incorporation of phosphate into the cellulose backbone significantly alters its properties by endowing the cellulose with phosphate characteristics. Cellulose phosphate was first developed to render cellulose-based textiles flame retardant (Ishizu, 1991; Reid, 1949). Cellulose phosphates have also been used as a cation-exchange material in the treatment of calcium-related diseases (Kennedy & Knil, 2003; Parfitt, 1975; Thomas Jr., 1978). Due to the ability of cellulose phosphate to induce the formation of calcium phosphate (mineralization process), it has the potential for use as an important implantable biomaterial in orthopedic applications (Fricain et al., 2001; Granja & Barbosa, 2001; Granja et al., 2001). The phosphate functionalities could also be used to bind various biologically active species to obtain specifically active surfaces (Granja et al., 2001; Leone, Torricelli, Giardino, & Barbucci, 2008).

Previous investigations regarding cellulose phosphate synthesis generally focused on the use of cotton or wood cellulose as the chemical feed-stock. However, cellulose is also available in large quantities from other non-woody plants such as flax, hemp, jute, bagasse, ramie, cereal straws, and oil palm biomass (OPB). OPB, a by-product of the oil palm industry, comes in various forms, e.g., empty fruit bunches (OPEFBs), fibers, shells, wet shells, palm kernels, fronds and trunks. In 2006, Malaysia alone produced about 70 million tons of oil palm biomass, including trunks, fronds, and empty fruit bunches (Yacob, 2007). These residues represent an abundant, inexpensive, and readily available source of renewable lignocellulosic biomass. Several processes, such as electricity generation (Biogen, 2008), conversion into pulp and paper (Wanrosli, Zainuddin, Law, & Asro, 2006) and production of roughage for animal feeds (MARDI, 2008), can transform OPB into value-added products. The high cellulose content of 60.6% in OPEFB (Wanrosli, Zainuddin, & Lee, 2004) represents a vast potential that could be exploited for high value-added products via conversion into cellulose derivatives, particularly cellulose phosphate, which is the aim of this investigation.

The standard method for cellulose isolation is delignifying the wood/plant material using acidified sodium chlorite (Wise, Murphy, & D'Addieco, 1946). However, because of environmental concerns associated with the use of chlorine and its derivatives, the cellulose in this study was prepared via a chlorine-free (TCF) bleaching sequence (Leh, Wan Rosli, Zainuddin, & Tanaka, 2008; Wan Rosli, Leh, Zainuddin, & Tanaka, 2003). Prior to phos-

* Corresponding author. Tel.: +60 4 653 2354; fax: +60 4 657 3678.
E-mail address: wanrosli@usm.my (W.D. Wanrosli).

0144-8617/$ – see front matter © 2010 Elsevier Ltd. All rights reserved.
doi:10.1016/j.carbpol.2010.11.032

phorylation, the isolated cellulose was further processed into microcrystalline cellulose (MCC), which is a purified, partially depolymerized cellulose prepared by treating high-quality cellulose with hydrochloric acid to the leveling-off the degree of polymerization (LODP) is reached (Battista, Coppick, Howsmon, Morehead, & Sisson, 1956).

OPEFB was chosen as the raw material for this investigation because of its abundance, accessibility and suitability. This paper reports the synthesis of cellulose phosphate (OPEFB-CP) from OPEFB-MCC by phosphorylation using the $H_3PO_4/P_2O_5/Et_3PO_4$ procedure. In view of the potential applicability of this material and the fact that it was prepared from an alternative non-woody source of cellulose, a thorough characterization of its physico-chemical properties was performed to determine the phosphorous content (using the Kjeldahl method), morphology (using scanning electron microscopy (SEM)), elemental content (energy dispersive X-ray (EDX) analysis), spectral properties (Fourier transform infrared (FTIR) analysis and nuclear magnetic resonance (CP/MAS ^{31}P and ^{13}C NMR)) and thermal properties (differential scanning calorimetry (DSC)).

2. Materials and methods

2.1. Preparation of oil palm empty fruit bunch microcrystalline cellulose

For this investigation, oil palm empty fruit bunch (OPEFB) cellulose was prepared using the environmentally benign process described by Wan Rosli et al. (2003) and Leh et al. (2008). This procedure involves water pre-hydrolysis of the OPEFB, followed by soda-anthraquinone pulping. Then the unbleached pulp was bleached using a totally chlorine-free (TCF) sequence of oxygen (O), ozone (Z) and peroxide (P) to a kappa number of 1.4. The bleached pulp was later hydrolyzed for the preparation of microcrystalline cellulose (MCC) with 2.5 M HCl while maintaining a solid to liquor ratio of 1:20 and refluxing at 105 ± 2 °C for 15 min. After the hydrolysis, the material was thoroughly washed with distilled water before air drying. Powdered OPEFB-MCC was then obtained by grinding the sample in a ball mill, and it was subsequently kept in a desiccator over phosphorous pentoxide before further use.

2.2. Synthesis of oil palm empty fruit bunch microcrystalline cellulose phosphate

The phosphorylation of cellulose was carried out using the method described by Granja et al. (2001). OPEFB MCC (4.0 g) was consecutively swollen in distilled water, ethanol and hexanol for 24 h each to activate the cellulose surface. The reaction was carried out in a four-neck round bottom flask equipped with a nitrogen inlet, condenser, thermometer, and mechanical stirrer. After dispersing the OPEFB-MCC in 29 mL of 1-hexanol, a solution of 50 g of phosphorus pentaoxide in 37 mL of triethylphosphate and 42 mL of 85% phosphoric acid was added portion-wise to the suspension. The reaction was allowed to proceed under constant stirring in a nitrogen atmosphere at various reaction temperatures and for various reaction times, as listed in Table 1. Then the product was washed with hexanol and ethanol to remove the excessive reagents. This method was chosen because cellulose phosphate used in biomaterials must be free of any biologically hazardous compounds that might be present after using other alternative techniques (Vigo & Welch, 1974). The OPEFB-CP was subsequently air-dried at room temperature and kept in a desiccator over phosphorous pentoxide before analysis.

Table 1
Effect of reaction parameters on the yield and degree of substitution of OPEFB-CP.

Sample No.	Reaction temperature (°C)	Reaction time (h)	% Yield	Degree of substitution (DS)
I	30	72	75	1.03
II	50	72	50	2.2
III	70	72	No yield	–
IV	50	120	<10	0.21
	Unmodified CMC			0

2.3. Determination of the degree of substitution

The degree of substitution (DS) was calculated according to the following equation (Towle & Whistler, 1972):

$$DS = \frac{162 \times \%P}{3100 - 84 \times \%P},$$

where $\%P$ is the phosphorous content.

Quantification of the phosphorous content requires the conversion of phosphorus to dissolved orthophosphate followed by colorimetric determination of the dissolved orthophosphate (Csuros, 1997). A sulfuric–nitric acid mixture is typically used as the oxidant for the Kjeldahl digestion procedure. After the sample was fully digested, it was analyzed using the ascorbic acid colorimetric method. In this particular approach, ammonium molybdate and antimony potassium tartrate were allowed to react in an acid medium with a diluted solution of phosphorous to form an antimony–phospho-molybdate complex. In the presence of ascorbic acid, it was reduced to a blue-colored solution that was proportional to the phosphorous concentration, which could then be spectrometrically determined at 760 nm.

2.4. Swelling capacity

To evaluate the swelling capacity, samples were allowed to soak in water in centrifuge polyethylene tubes for 30 min, followed by centrifugation at 5000 rpm for 15 min. After removal of excess water, the samples were weighed again. The swelling capacity was determined via the difference between the weights before and after swelling.

$$\textit{Swelling capacity}\,(\%) = \frac{W_i - W_o}{W_o} \times 100,$$

where W_i and W_o are the weights of the dry and swollen samples, respectively.

2.5. Characterization methods

The scanning electron microscopy and EDX elemental analyses were carried out using a SEM-EDX Oxford INCA 400 model. FTIR was performed on a Nicolet Avatar 360 using the KBr method. Solid-state ^{31}P magic angle spinning (MAS) and ^{13}C cross polarization (CP) CP/MAS measurements were carried out using a Bruker Avance 600 MHz NMR operating at 75.5 MHz (^{13}C NMR) and 121.5 (^{31}P NMR) with external reference standards of tetramethylsilane and 85% H_3PO_4, respectively. In all instances, the MAS rate was 7.0 kHz. DSC thermograms were obtained using a Perkin Elmer DSC6 with approximately 3 mg of material in sealed aluminum pans that were heated from ambient temperature to 350 °C at a heating rate of 10 °C/min under a flowing nitrogen atmosphere.

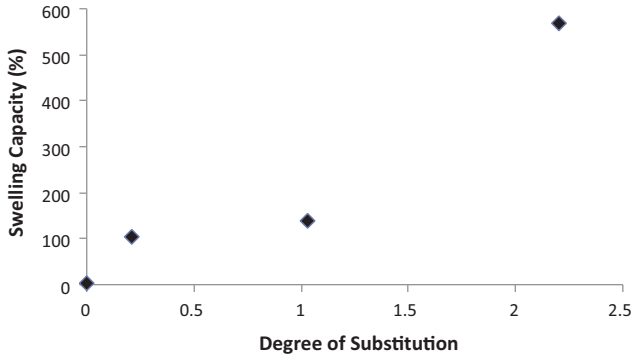

Fig. 1. Relationship between the swelling capacity and degree of substitution of OPEFB-CP.

3. Results and discussion

3.1. Synthesis of oil palm empty fruit bunch cellulose phosphate

The phosphorylation of OPEFB-MCC was carried out using the $H_3PO_4/P_2O_5/Et_3PO_4$/hexanol method. Depending on the reaction conditions, a substantially high yield and high degree of cellulose phosphate gel substitution were obtained (see Table 1). Nevertheless, it could be seen that, although the DS increased with temperature (from 30 to 50 °C), no product was obtained at the highest temperature investigated (70 °C), presumably due to product degradation. The swelling of the cellulose matrix increased at higher temperatures as a result of a greater number of hydrogen bonds being broken. Thus, the phosphorylating agents had better access to the matrix, which in turn enhanced the reaction rate, as implied by the DS results. During any chemical reaction involving cellulose, the reactants diffuse into the inner layer of the cellulose fiber, which break intra- and intermolecular bonds and degrade the crystalline region of the fiber. Thus, more active and accessible hydroxyl groups are available for reaction (Obataya & Minato, 2007), which increases the DS. However, with further increases in temperature, the competitive reactions of phosphorylation and the hydrolysis of pre-existing phosphoester bonds tend to favor the latter reaction (Granja et al., 2001), resulting in a severely degraded cellulose phosphate (sample III). Consequently, only a negligible amount of product was obtained at high temperatures. Prolonging the reaction time (samples II and IV) was also detrimental; both the yield and DS decreased dramatically due to the degradation of the OPEFB-CP formed. Based on these considerations, a reaction temperature and time of 50 °C and 72 h, respectively, were considered the optimum conditions for the synthesis of OPEFB-CP with a DS of 2.2 for further characterization.

In terms of swelling, phosphorylated MCC absorbed substantially more water than the unmodified MCC, with increasing absorption at higher DS (Fig. 1). This increase is partly due to the reduction in the degree of crystallinity (see Section 3.4) and thus greater accessibility of the water hydroxyl groups as a result of phosphorylation. Furthermore, the introduction of phosphate groups onto the cellulose backbone increased the possibility of attaching more water molecules via hydrogen bonding.

3.2. Morphology and elemental analysis

The morphological structures of OPEFB-MCC and OPEFB-CP as observed using SEM are shown in Fig. 2a and b, respectively. Upon phosphorylation, the OPEFB-CP became gel-like, and the texture was more compact compared to that of the native OPEFB-MCC. The elemental analysis determined by EDX confirmed the presence of phosphorous with an 11.9% increase in P upon phosphorylation. In addition, there was also a 2.1% increase of O due to the substitution of OH groups by the phosphate groups, which contained two additional O atoms.

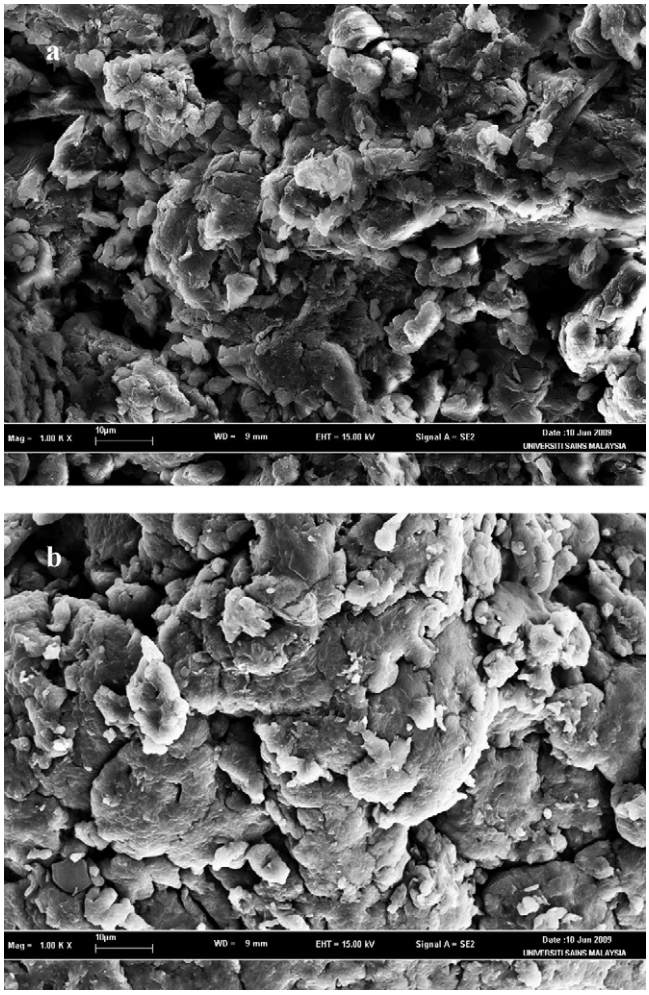

Fig. 2. SEM micrographs of (a) native OPEFB-MCC and (b) OPEFB-CP with DS = 2.2.

3.3. FTIR spectral analysis

Fig. 3 shows the FTIR spectra for both the OPEFB MCC and its phosphorylated form. The spectrum for OPEFB-MCC (Fig. 3a) is similar to that of pure cellulose as reported by Zhbankov (1966) and exhibited the vibration band characteristics of the –OH stretching vibration around 3700–3200 cm^{-1}, –OH in-plane deformation between 1450–1320 cm^{-1} and C–O stretching vibrations from 1165 to 1050 cm^{-1}. After phosphorylation, several new absorption peaks characteristic of cellulose phosphate emerged, the vibration bands of P=O at 1377 cm^{-1}, P–H at 2385 cm^{-1} and C–O–C at 1021 cm^{-1} (Fig. 3b) (Kaputskii & Komar, 1988). In addition, there was a clear reduction in the –OH stretching vibration in the cellulose spectrum (3700–3200 cm^{-1}), which indicated the conversion of the cellulose hydroxyl groups into phosphate groups during phosphorylation. A considerable shift of this peak to higher frequencies was also observed, which was most likely due to the changes in the pattern and distribution of the hydrogen bonds caused by the introduction of the phosphate groups.

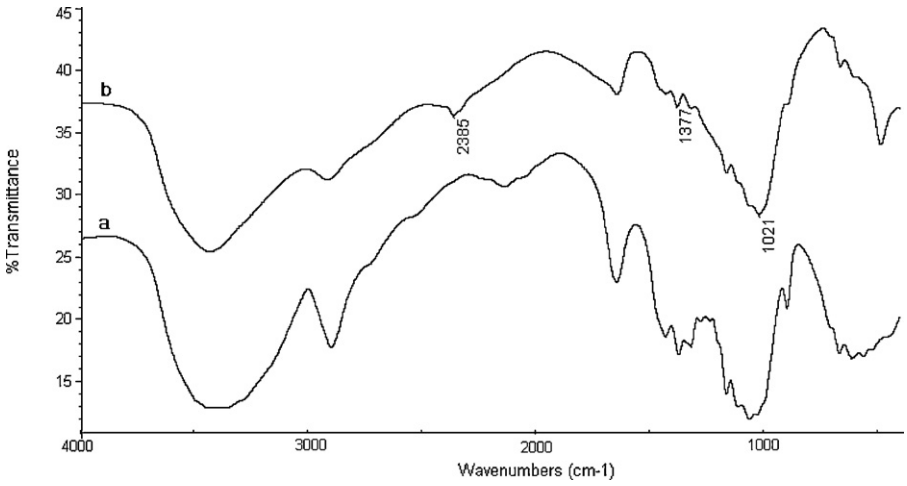

Fig. 3. FTIR spectra of (a) native OPEFB-MCC and (b) OPEFB-CP with DS = 2.2.

3.4. NMR analysis

The FTIR findings on the structure of the OPEFB cellulose phosphate were corroborated by the solid state results of ^{31}P-NMR/MAS (Fig. 4). The occurrence of a signal at δ 0.88 ppm, which is associated with phosphate functionalities (Kuhl, 2008; Sabesan & Neira, 1992; Srivastava & Hindsgaul, 1985), further confirmed that the phosphorylation reaction had occurred. The two symmetrical side bands at ±58 ppm were rotational side bands resulting from powder anisotropy (Granja et al., 2001).

To provide further information on the structure of cellulose phosphate from OPEFB, ^{13}C-NMR/MAS solid state analysis was performed, and the full spectra of both OPEFB-MCC (spectrum a) and OPEFB-CP (spectrum b) are shown in Fig. 5. The resonance lines in OPEFB-MCC were assigned to the carbons of C1 (105.4 ppm) and C4 (88.3 ppm), and a cluster of resonances at 70–80 ppm belonged to the C2, C3 and C5 carbons (Love, Snape, & Jarvis, 1998; Newman & Hemmingson, 1995; Newman, 1998; Wickholm, Larsson, & Iversen, 1996). Nevertheless, the expected C6 peak of approximately 63 ppm was not well resolved, and it appeared as a shoulder. Upon phosphorylation, three resonance lines appeared at ca. 104.8, 75.0 and 63.0 ppm, which could be respectively attributed to the shifted C1, C2–5 and C6 carbons of the cellulose phosphate (Granja et al., 2001). The occurrence of chemical shifts indicated the phosphorylation of the OPEFB-MCC. The most noticeable shifts were the C2, C3 and C5 peaks from 74.45 to 75.02 ppm and the C1 peak from 105.42 to 104.8 ppm. The downfield shift of the former was due to the de-shielding effect following the phosphorylation of its hydroxyl group because de-shielding occurs when hydroxyl groups of simple polysaccharides are esterified (Capon, Rycroft, & Thomson, 1979). However, the upfield shift of the latter was a consequence of the anisotropic shielding effects resulting from the phosphorylation of the neighboring hydroxyl group at C2. In addition, there were two new additional features observed, as shown in Fig. 4. After phosphorylation, the previously unresolved C6 line in OPEFB-MCC was well resolved (63.1 ppm), suggesting that phosphorylation predominantly occurred on C6, which was expected because it was the least sterically hindered of all available hydroxyl groups in the glucose moiety. The absence of any splitting of the C6 line as suggested by Granja et al. (2001) and of any broad peak (Yamamoto, Horii, & Hirai, 2006) indicated a major conversion of the hydroxyl groups in this position. The second observation was the disappearance of the C4 line in the OPEFB-CP, which then formed part of the shoulder of the resonances of

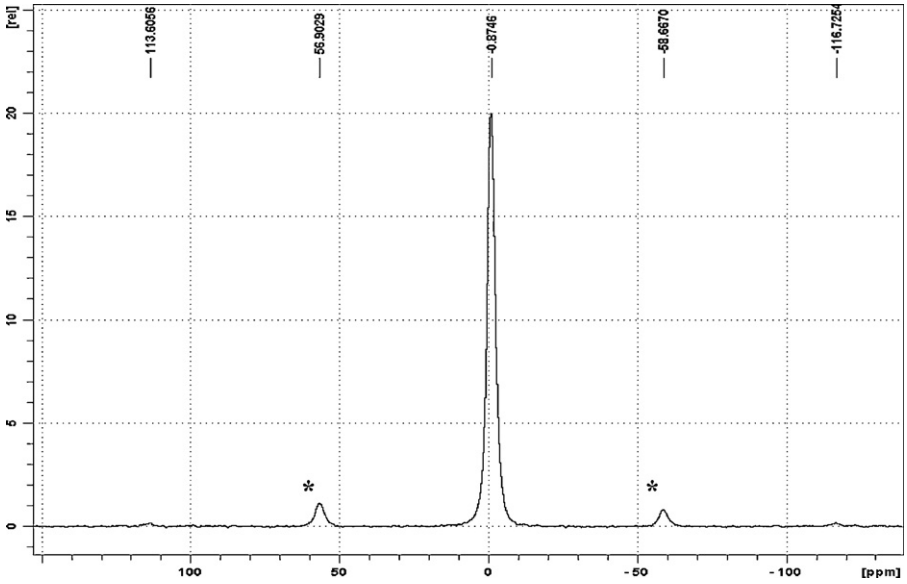

Fig. 4. CP/MAS ^{31}P-NMR spectrum of OPEFB-CP with DS = 2.2. Side bands are shown as asterisks (*), and 85% H_3PO_4 was used as the reference standard.

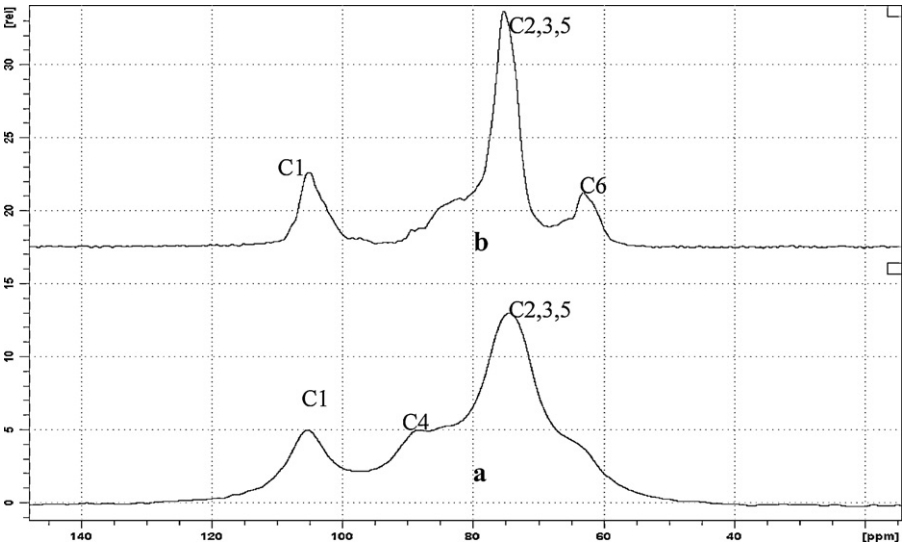

Fig. 5. CP/MAS ^{13}C-NMR spectra of (a) native OPEFB-MCC and (b) OPEFB-CP with DS = 2.2. TMS was used as the reference standard.

the C2, C3 and C5 carbons. This disappearance could have been due to the shielding effects that arose from substitution on the C3 neighboring atom (beta effect), which created an upfield shift of the C4 resonance that overlapped onto the C2, C3 and C5 lines. Similar findings were reported by Takahashi, Fujimoto, Barua, Miyamoto, & Inagaki (1986) while investigating the ^{13}C-NMR spectra of cellulose derivatives.

The introduction of phosphate groups onto the cellulose backbone also disrupted the crystalline structure and reduced the crystallinity of the cellulose, which was confirmed by the crystallinity index (CrI) of 0.19 in OPEFB-CP, compared to 0.40 in OPEFB-MCC, as estimated from the integrals of the C4 signals centered at 87–93 ppm and 80–87 ppm, which represented the crystalline and amorphous regions of the cellulose, respectively (Ek, Wormald, Jan östelius, & Nyström, 1995).

3.5. Thermal analysis

The effects of phosphorylation on the thermal properties of OPEFB-MCC were examined using differential scanning calorimetry (DSC), and the results are shown in Fig. 6.

Cellulosic materials usually have a strong affinity for water because of the presence of non-substituted hydroxyl groups and the crystallinity of the material. Cellulose is composed of amorphous and crystalline regions (Saka, 2004). In the amorphous regions, the cellulose chains are packed loosely, leading to greater accessibility of the water molecules compared to the crystalline region. In addition, the availability of the non-substituted hydroxyl groups in the amorphous region is greater than that in the crystalline region due to fewer intra- and intermolecular bonds. Thus, the lower the cellulose crystallinity is, the higher the water absorption.

In the DSC thermogram, a pronounced peak appeared in the range of 30–120 °C, which was associated with the loss of water due to evaporation (Scandola & Ceccorulli, 1985). A close inspection of the thermograms suggested that there was a considerable shift in the position of the maximum peak temperature between OPEFB-MCC and its phosphorylated form, with the former occurring at 72.3 °C and the latter at 86.3 °C. Thus, these polymers differed in terms of water holding capacity and water-polymer interaction. The peak areas of the endotherms also differed, with a higher ΔH for OPEFB-CP (218.4 J/g vs. 153.8 J/g for OPEFB-MCC). Both of these differences were further indications of the changes that occurred in the chemical and physical properties of OPEFB-MCC during phos-

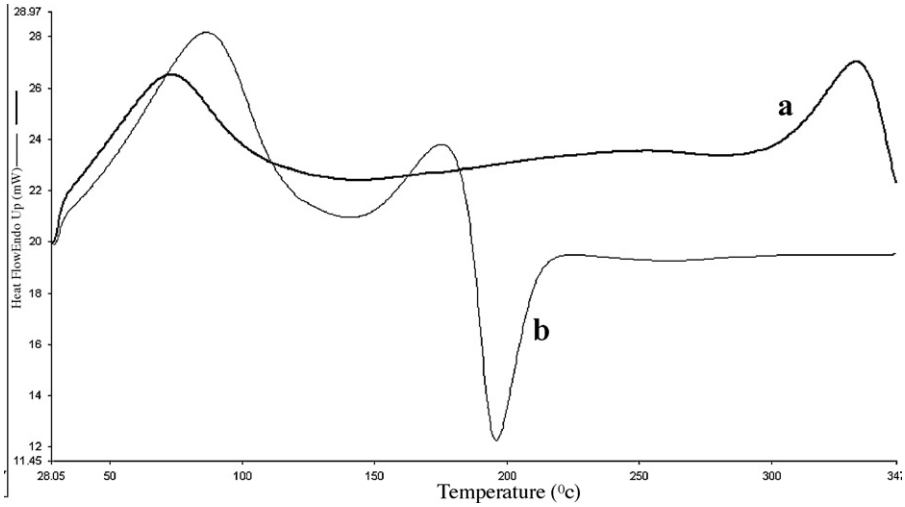

Fig. 6. DSC thermograms of (a) native OPEFB-MCC and (b) OPEFB-CP with DS = 2.2.

phorylation. The water molecules in OPEFB-MCC are held together by the cellulosic hydroxyl groups. However, after phosphorylation, the hydroxyl groups were replaced by phosphate groups, which are capable of binding more water molecules through the formation of new hydrogen bonds, thus increasing the bound water content. Phosphorylation was also observed to decrease the crystallinity of OPEFB-MCC as discussed earlier, which increased the water holding capacity of the phosphorylated OPEFB-MCC. Two endotherms appeared in the OPEFB-MCC thermogram with peak temperatures of 233 °C and 333 °C and were therefore associated with the thermal depolymerization processes of cellulose (Soares, Camino, & Levchik, 1995). These were replaced by an exotherm in the OPEFB-CP thermogram with a peak temperature of 195.4 °C, corresponding to the decomposition of the OPEFB-CP and indicating that the latter was less thermally stable. The thermal instability of OPEFB-CP was possibly due to the reduced crystallinity of the product as a consequence of phosphorylation, as discussed earlier. Similar changes have been observed in cellulose with an increased amorphous content (Cabradilla & Zeronian, 1978).

4. Conclusions

Cellulose phosphate gel was successfully synthesized from OPEFB-MCC using the $H_3PO_4/P_2O_5/Et_3PO_4$/hexanol method. The temperature influenced the yield and quality more than the reaction time. Phosphorylation reaction confirmation was performed with FTIR, CP/MAS ^{13}C-NMR, and ^{31}P-NMR spectroscopic analyses as well as EDX analysis. CP/MAS ^{13}C NMR showed that the OH group on C6 was subjected to a higher preferential phosphorylation than the OH groups on C2 and C3, and there was a concomitant reduction in crystallinity of 53%. DSC thermograms showed both the hydration temperature and its associated ΔH for OPEFB-CP to be different from those properties of the native OPEFB-MCC, which provided further indication of phosphorylation.

Acknowledgements

The financial support from Universiti Sains Malaysia through Research University Grant No. 1001/PTEKIND/8140151 is gratefully acknowledged, and we would like to thank Mr. Kun Cheng of SUNY-ESF for performing the NMR analysis.

References

Battista, O. A., Coppick, S., Howsmon, J. A., Morehead, F. F., & Sisson, W. A. (1956). Level-off degree of polymerization. *Industrial and Engineering Chemistry*, *48*, 333–335.

Biogen (2008). Keck Seng (M) Berhad. http://www.biogen.org.my/bris/BioGen/Tech.

Cabradilla, K. E., & Zeronian, S. H. (1978). Effect of changes in supramolecular structure on the thermal properties and pyrolysis of cellulose. In R. M. Rowell, & R. A. Young (Eds.), *Modified cellulosics* (pp. 321–340). New York: Academic Press.

Capon, B., Rycroft, D. S., & Thomson, J. W. (1979). The ^{13}C NMR spectra of peracetylated cello-oligosaccharides. *Carbohydrate Research*, *70*, 145–149.

Csuros, M. (1997). *Environmental sampling and analysis*. Lab Manual: CRC Press.

Dumitru, S. (2002). Polysaccharides as biomaterials. In S Dumitru (Ed.), *Polymeric biomaterials* (2nd ed., pp. 1–63). New York: Markel Dekker.

Ek, R., Wormald, P., Jan östelius, I. T., & Nyström, C. (1995). Crystallinity index of microcrystalline cellulose particles compressed into tablets. *International Journal of Pharmaceutics*, *125*, 257–264.

Fricain, J. C., Granja, P. L., Barbosa, M. A., de Jeso, B., Barthe, N., & Baquey, C. (2001). Cellulose phosphates as biomaterials. In vivo biocompatibility studies. *Biomaterials*, *23*, 971–980.

Granja, P. L., & Barbosa, M. A. (2001). Cellulose phosphates as biomaterials. Mineralization of chemically modified regenerated cellulose hydrogels. *Journal of Materials Science*, *36*, 2163–2172.

Granja, P. L., Pouysegu, L., Petraud, M., De Jeso, B., Baquey, C., & Barbosa, M. A. (2001). Cellulose phosphates as biomaterials. I. Synthesis and characterization of highly phosphorylated cellulose gels. *Journal of Applied Polymer Science*, *82*, 3341–3353.

Hon, D. N.-S. (1996). Cellulose and its derivatives: Structures reactions and medical uses. In S. Dumitriu (Ed.), *Polysaccharides in medicinal applications* (pp. 87–105). New York: Markel Dekker.

Ishizu, A. (1991). Chemical modification of cellulose. In D. N.-S Hon, & N. Shiraishi (Eds.), *Wood and cellulose chemistry* (pp. 757–800). Marcel Dekker: New York.

Kaputskii, V. E., & Komar, V. P. (1988). Infrared spectra and structure of cellulose phosphate. *Zhurnal Prikladnoi Spektroskopii*, *48*, 257–262.

Kennedy, J. F., & Knil, C. J. (2003). Biomaterials utilised in medical textiles: An overview. In S. C. Anand, J. F. Kennedy, M. Miraftab, & S. Rajendran (Eds.), *Medical textiles and biomaterials for healthcare* (pp. 3–22). England: Woodhead Publishing Limited.

Kuhl, O. (2008). *Phosphoros-31 NMR spectroscopy*. Berlin Heidelberg: Springer-Verlag.

Leh, C. P., Wan Rosli, W. D., Zainuddin, Z., & Tanaka, R. (2008). Optimization of oxygen delignification in production of totally chlorine free cellulose pulps from oil palm empty fruit bunch fiber. *Industrial Crops and Products*, *28*, 260–267.

Leone, G., Torricelli, P., Giardino, R., & Barbucci, R. (2008). New phosphorylated derivatives of carboxymethylcellulose with osteogenic activity. *Polymers for Advanced Technologies*, *19*, 824–830.

Love, G. D., Snape, C. E., & Jarvis, M. C. (1998). Comparison of leaf and stem cell-wall components in barley straw by solid-state ^{13}C NMR. *Phytochemistry*, *49*, 1191–1194.

MARDI (2008). Malaysian Agricultural Research and Development Institute. http://www.mardi.my.

Newman, R. H. (1998). Evidence for assignment of ^{13}C NMR signals to cellulose crystallite surfaces in wood pulp and isolated celluloses. *Holzforschung*, *52*, 157–159.

Newman, R. H., & Hemmingson, J. A. (1995). Carbon-13 NMR distinction between categories of molecular order and disorder in cellulose. *Cellulose*, *2*, 95–110.

Obataya, E., & Minato, K. (2007). Effects of previous solvent exchange on acetylation of wood. *Wood Science and Technology*, *41*, 351–360.

Parfitt, A. M. (1975). Effect of cellulose phosphate on calcium and magnesium homeostasis: Studies in normal subjects and patients with latent hypoparathyroidism. *Clinical Science and Molecular Medicine*, *49*, 83–90.

Reid, J. D., & Mazzeno, L. W., Jr. (1949). Preparation and properties of celulose phosphates. *Industrial and Engineering Chemistry*, *41*, 2828–2831.

Sabesan, S., & Neira, S. (1992). Synthesis of glycosyl phosphates and azides. *Carbohydrate Research*, *223*, 169–185.

Saka, S. (2004). Wood as raw materials for cellulose acetate production. *Macromolecular Symposia*, *208*, 7–28.

Scandola, M., & Ceccorulli, G. (1985). Viscoelastic properties of cellulose derivatives: 1. Cellulose acetate. *Polymer*, *26*, 1953–1957.

Soares, S., Camino, G., & Levchik, S. (1995). Comparative study of the thermal decomposition of pure cellulose and pulp paper. *Polymer Degradation and Stability*, *49*, 275–283.

Srivastava, O. P., & Hindsgaul, O. (1985). Synthesis of glycosides of α-D-mannopyranose 6-(α-D-glucopyranosyl phosphate). The putative ligatin receptor. *Carbohydrate Research*, *143*, 77–84.

Takahashi, S. I., Fujimoto, T., Barua, B. M., Miyamoto, T., & Inagaki, H. (1986). ^{13}C-NMR spectral studies on the distribution of substituents in some cellulose derivatives. *Journal of Polymer Science Part A: Polymer Chemistry Edition*, *24*, 2891–2993.

Thomas, W. C., Jr. (1978). Use of phosphates in patients with calcareous renal calculi. *Kidney International*, *13*, 390–396.

Towle, G. A., & Whistler, R. L. (1972). Phosphorylation of starch and cellulose with an amine salt of tetrapolyphosphoric acid. In R. L. Whistler (Ed.), *Methods of carbohydrate chemistry* (pp. 408–411). New York: Academic Press.

Vigo, T. L., & Welch, C. M. (1974). Chlorination and phosphorylation of cotton cellulose by reaction with phosphoryl chloride in *N*,*N*-dimethylformamide. *Carbohydrate Research*, *32*, 331–338.

Wan Rosli, W. D., Leh, C. P., Zainuddin, Z., & Tanaka, R. (2003). Optimisation of soda pulping variables for preparation of dissolving pulps from oil palm fiber. *Holzforschung*, *57*, 106–113.

Wanrosli, W. D., Zainuddin, Z., & Lee, L. K. (2004). Influence of pulping variables on the properties of Elaeis guineensis soda pulp as evaluated by response surface methodology. *Wood Science and Technology*, *38*, 191–205.

Wanrosli, W. D., Zainuddin, Z., Law, K. N., & Asro, R. (2006). Pulp from oil palm fronds by chemical processes. *Industrial Crops and Products*, *25*, 89–94.

Wickholm, K., Larsson, P. T., & Iversen, T. (1996). Assignment of non-crystalline forms in cellulose I by CP/MAS ^{13}C NMR spectroscopy. *Carbohydrate Research*, *312*, 123–129.

Wise, L. E., Murphy, M., & D'Addieco, A. A. (1946). Chlorite holocellulose, its fractionation and bearing on summative wood analysis and on studies on the hemicelluloses. *Paper Trade*, *122*, 35–43.

Yacob, S. (2007). Progress and challenges in utilization of oil palm biomass. In Paper presented at Asian Science and Technology Seminar, sponsored by Japan Science and Technology Agency, 8–9 March, Jakarta, Indonesia.

Yamamoto, H., Horii, F., & Hirai, A. (2006). Structural studies of bacterial cellulose through the solid-phase nitration and acetylation by CP/MAS ^{13}C NMR spectroscopy. *Cellulose*, *13*, 327–342.

Zhbankov, R. G. (1966). *Infrared spectra of cellulose and its derivatives*. New York: Consultants Bureau, Plenum Publishing Corporation.